

第八届全国重味物理与量子色动力学研讨会

D_{s1} 的 $D_s \pi \pi$ 衰变和 $T_{c\bar{s}}$ 粒子的耦合道解释

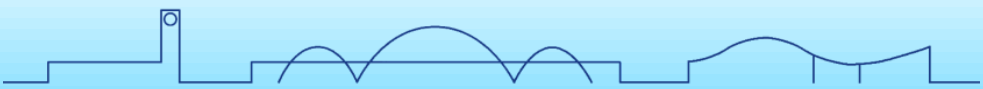
Jia-jun Wu (UCAS)

Collaborator: Guangjuan Wang (KEK), Zhi Yang (USETC), Makoto Oka (RIKEN),
Shi-lin Zhu (PKU)

PRL 128 (2022) 112001, 2510.01564

重庆大学

2026.04.25



中国科学院大学
University of Chinese Academy of Sciences



Outline

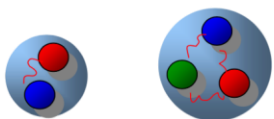
- Background: Bare state + Coupled channel
- NPHF
- From $D_s(2317)$ to $T_{c\bar{s}}(2327)$
- Summary and Outlook



Background: Beyond Quark Model

Hadron state:
meson, baryon//Exotic

conventional hadron



(q q̄)

(qqq)

Quark
model?

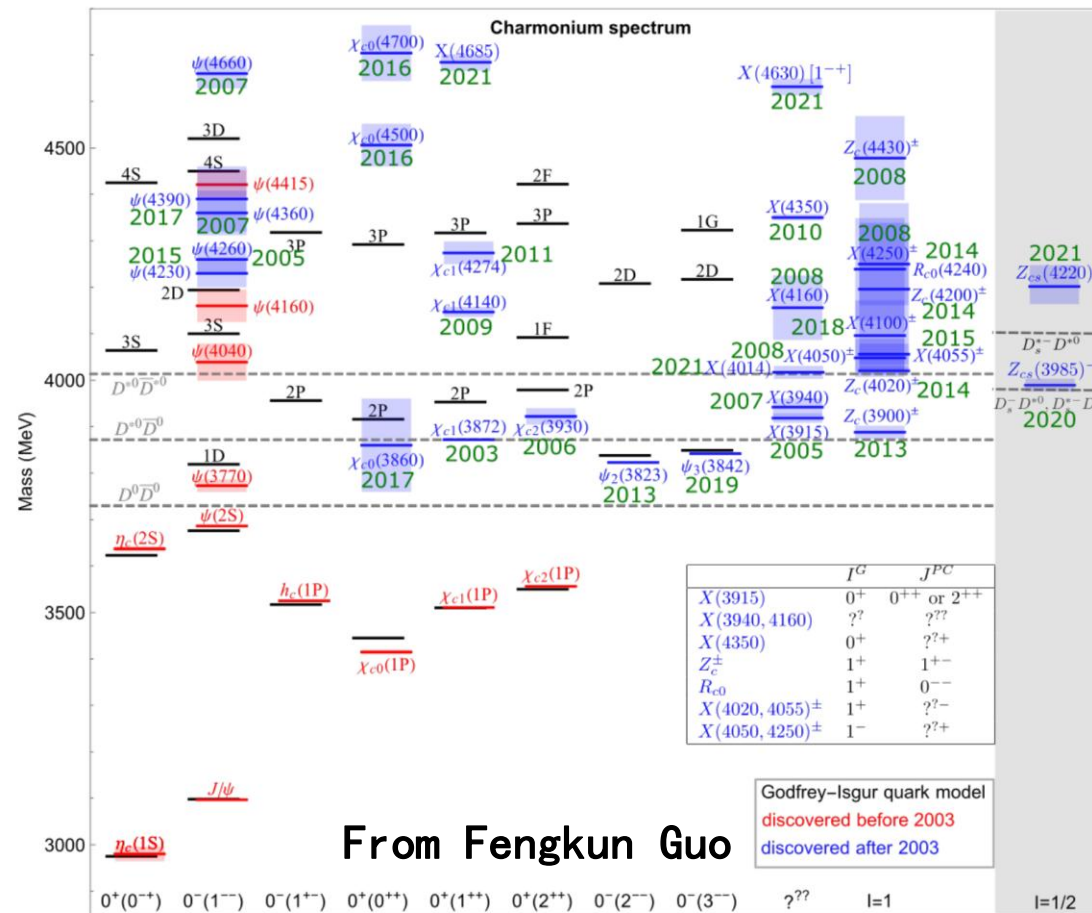
Quark/Gluon

Exotic

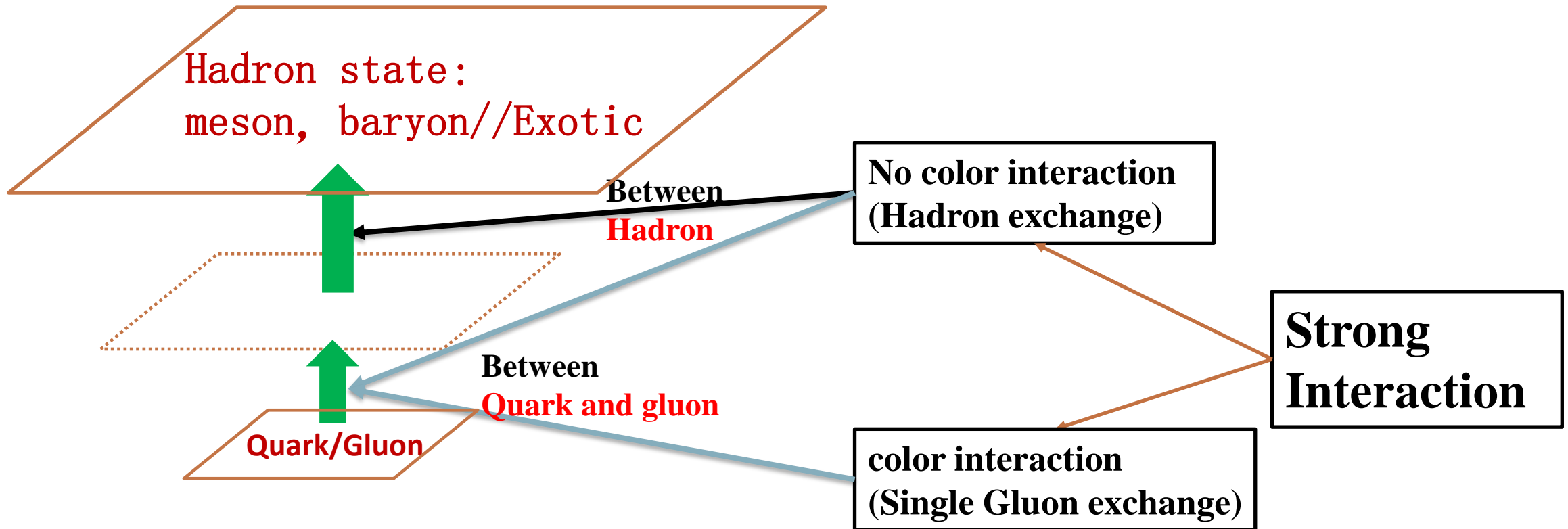
Hybrid Glueball Tetraquark



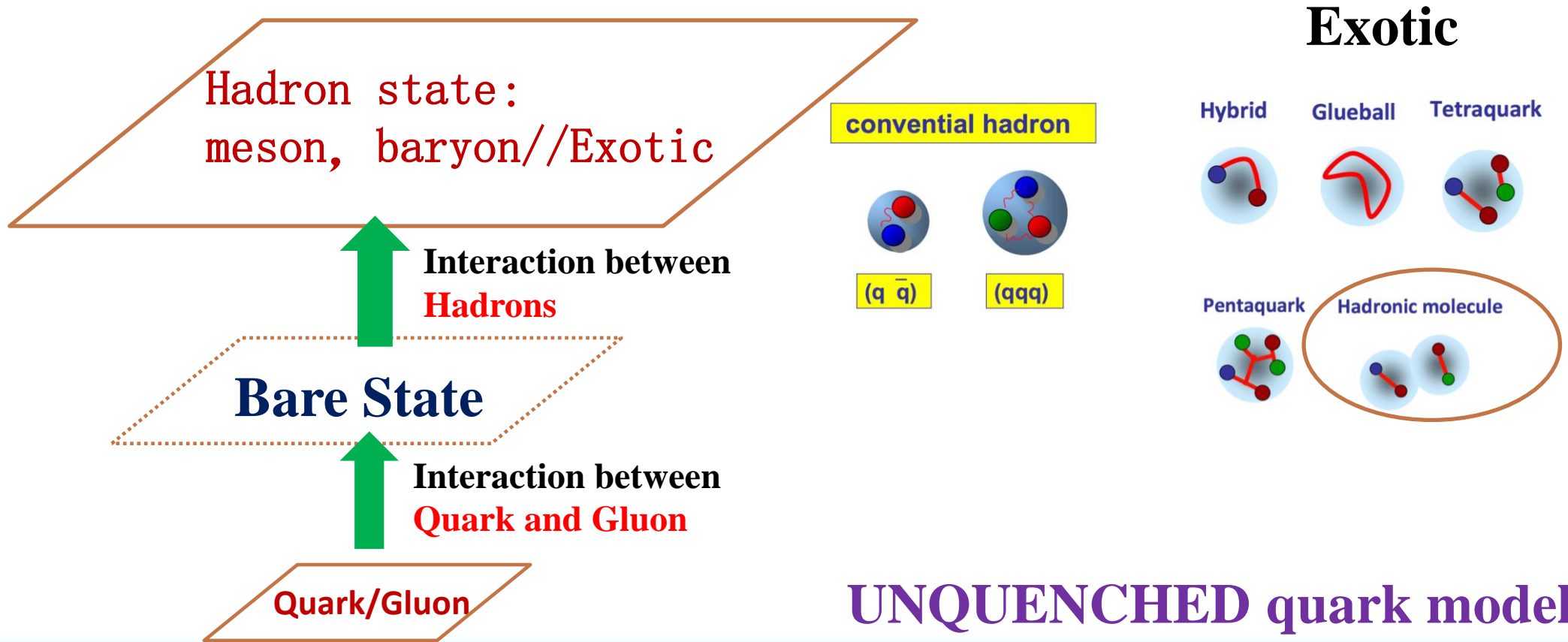
Pentaquark Hadronic molecule



Background: Strong Interaction



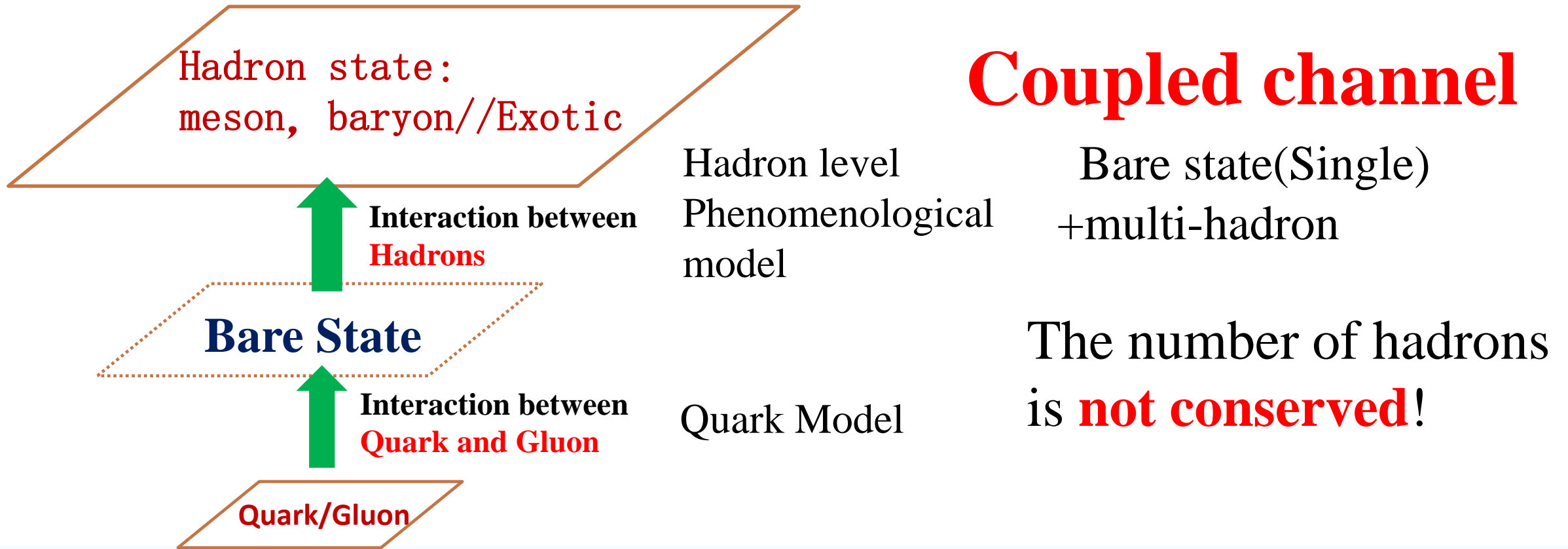
Background: Bare state + Coupled channel



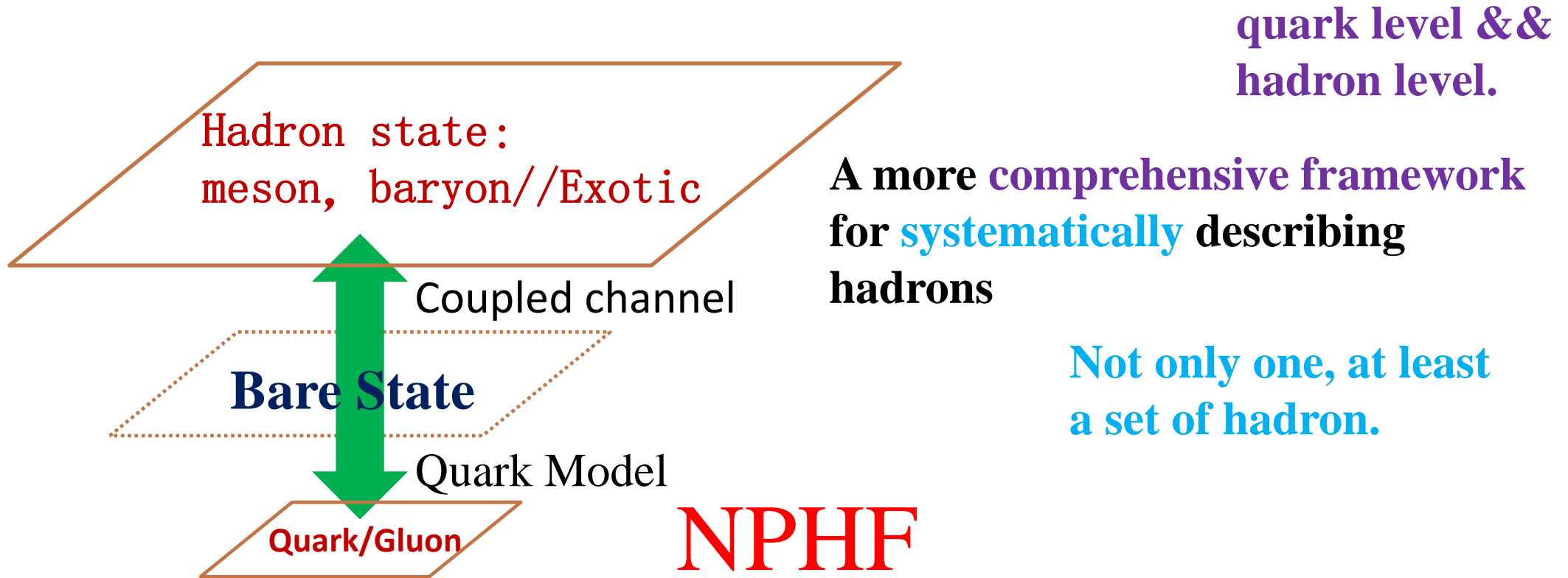
UNQUENCHED quark model



Background: Bare state + Coupled channel



Background: Strong-Spectrum-Reaction



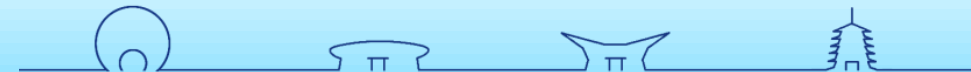
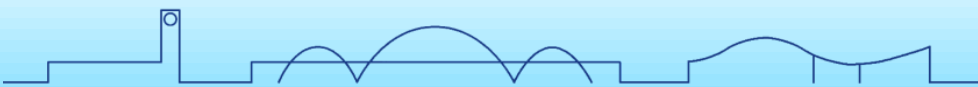
quark level &&
hadron level.

A more comprehensive framework
for **systematically** describing
hadrons

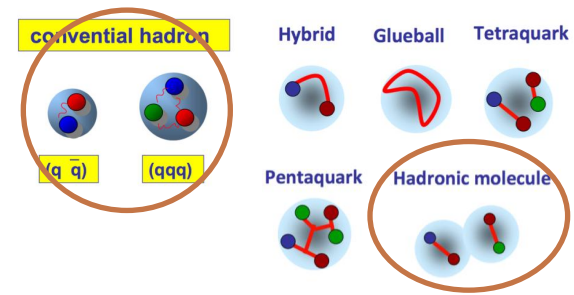
Not only one, at least
a set of hadron.

NPHF

NonPerturbative Hamiltonian Framework



NPHF: bare state + hadron channel



$$H = H_0 + H_I$$

$$H_0 = \sum_{i=1,n} |B_i\rangle m_i \langle B_i| + \sum_{\alpha} |\alpha(k_{\alpha})\rangle \left[\sqrt{m_{\alpha 1}^2 + k_{\alpha}^2} + \sqrt{m_{\alpha 2}^2 + k_{\alpha}^2} \right] \langle \alpha(k_{\alpha})|$$

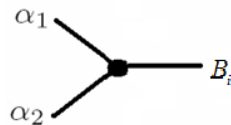
$|B_i\rangle$ bare state, bare mass m_i ↔ Quark level

$|\alpha(k_{\alpha})\rangle$ non-interaction channels ↔ Hadron level

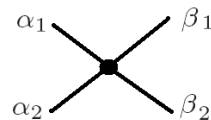
$$H_I = \hat{g} + \hat{v}$$

$$\hat{g} = \sum_{\alpha} \sum_{i=1,n} \left[|\alpha(k_{\alpha})\rangle g_{i,\alpha}^+ \langle B_i| + |B_i\rangle g_{i,\alpha} \langle \alpha(k_{\alpha})| \right]$$

$$\hat{v} = \sum_{\alpha,\beta} |\alpha(k_{\alpha})\rangle v_{\alpha,\beta} \langle \beta(k_{\beta})|$$



From 3P0 model, and the wavefunction of quark model



One boson exchange (OBE)

T matrix
(phase shift, inelasticity)

Lattice spectrum

Resonance
(Mass, width, pole position, coupling)

Hamiltonian

1. Finite-volume matrix Hamiltonian model for a $\Delta \rightarrow N\pi$ system [PRD 87 \(2013\) no.9, 094510](#)
2. Finite-volume Hamiltonian method for coupled-channels interactions in lattice QCD [PRC 90 \(2014\) no.5, 055206](#)
3. Lattice QCD Evidence that the $\Lambda(1405)$ Resonance is an Antikaon-Nucleon Molecule [PRL 114 \(2015\) no.13, 132002](#)
4. Hamiltonian effective field theory study of the $N^*(1535)$ resonance in lattice QCD [PRL 116 \(2016\) no.8, 082004](#)
5. Hamiltonian effective field theory study of the $N^*(1440)$ resonance in lattice QCD [PRD 95 \(2017\) no.3, 034034](#)
6. Structure of the $\Lambda(1405)$ from Hamiltonian effective field theory [PRD 95 \(2017\) no.1, 014506](#)
7. Nucleon resonance structure in the finite volume of lattice QCD [PRD 95 \(2017\) no.11, 114507](#)
8. Structure of the Roper Resonance from Lattice QCD Constraints [PRD 97\(2018\) no.9, 094509](#)
9. Kaonic Hydrogen and Deuterium in Hamiltonian Effective Field Theory [PLB 808\(2020\),135652](#)
10. Partial Wave Mixing in Hamiltonian Effective Field Theory [PRD 101\(2020\) no.11,114501](#)
11. Hamiltonian effective field theory in elongated or moving finite volume [PRD 103\(2021\) no.9, 094518](#)
12. Regularization in Nonperturbative Extensions of Effective Field Theory [PRD 106 \(2022\) no.3, 034506](#)
13. Novel Coupled Channel Framework Connecting the Quark Model and Lattice QCD for the Near-threshold D_s States [PRL128\(2022\),112001](#)
14. The investigations of the P-wave B_s states combining quark model and lattice QCD in the coupled channel framework [JHEP01 \(2023\) 058](#)
15. Effects of multiple single-particle basis states in scattering systems [Annals Phys. 459\(2023\) 169531](#)
16. Low-lying odd-parity nucleon resonances as quark-model like states [PRD 108 \(2023\) 9, 094519](#)
17. Structure of the $\Lambda(1670)$ resonance [PRD 109 \(2024\) 5, 054025](#)
18. Investigation on the bottom analogs T_{bb} of T_{cc} [PRD 110 \(2024\) 7, 074007](#)
19. Pion photoproduction of nucleon excited states with Hamiltonian effective field theory [PRD 110 \(2024\) 9, 094015](#)
20. Study of the pion-mass dependence of ρ -meson properties in lattice QCD [PRD 109 \(2024\) 3, 034505](#)
21. Searching for the first radial excitation of the $\Delta(1232)$ in lattice QCD [JPG 51 \(2024\) 6, 065106](#)
22. Three-coupled-channel analysis of $Z_c(3900)$ involving DD^* , $\pi J/\psi$, and $\rho\eta_c$ [PRD 110 \(2024\) 11, 114029](#)
23. New insight into the exotic states strongly coupled with the DD^* from the T_{cc} [Sci.Bull. 69 \(2024\) 3036-3042](#)
24. Generalized boost transformations in finite volumes and application to Hamiltonian methods [JHEP 08 \(2024\) 178](#)
25. Spectral parameters of the ρ resonance from lattice QCD [JHEP 08 \(2025\) 064](#)
26. Finite volume Hamiltonian method for two-particle systems containing long-range potential on the lattice [JHEP 04 \(2025\) 108](#)
27. Structure of the $\Omega(2012)$ with Hamiltonian effective field theory [PRD 112 \(2025\) 5, L051503](#)
28. Nucleon resonance structure up to 2 GeV and the nature of the Roper resonance [PRD 111 \(2025\) 11, 116002](#)
29. Exploring the Ω^- spectrum in lattice QCD [JPG 52 \(2025\) 6, 065103](#)
30. The odd-parity strange baryons $\Sigma(1/2^-)$ below 1.8 GeV with Hamiltonian effective field theory [2509.17510](#)

$N^*(1440), N^*(1535), N^*(1650), N^*(1710), \Delta(1232), \Delta(1600), \Lambda(1405), \Lambda(1670),$
 $D_{s0}(2317), D_{s1}(2460), D_{s1}(2536), D_{s2}(2573), X(3872), T_{cc}, Z_c(3900), \dots$

NPHF

Resonance

(Mass , Width, Pole position, Coupling)

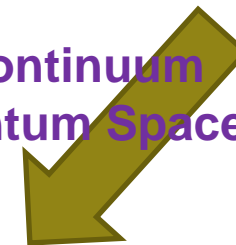


Complex Continuum
Momentum Space

Hamiltonian

Real Continuum
Momentum Space

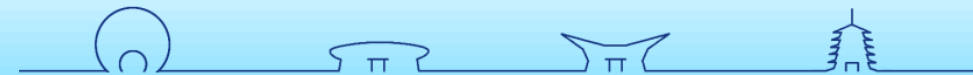
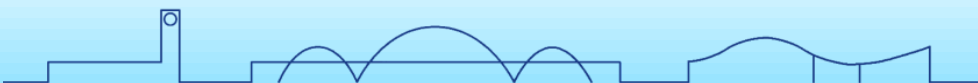
Real Discrete
Momentum Space



T matrix

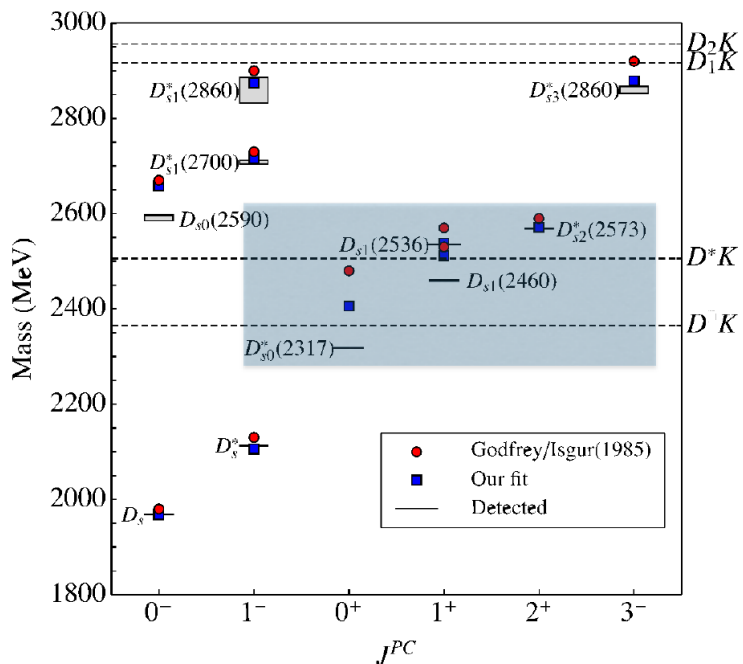
(Phase Shifts,
inelasticity)

Lattice Spectrum



$D_{s0}(2317)$, $D_{s1}(2460)$, $D_{s1}(2536)$, $D_{s2}(2573)$

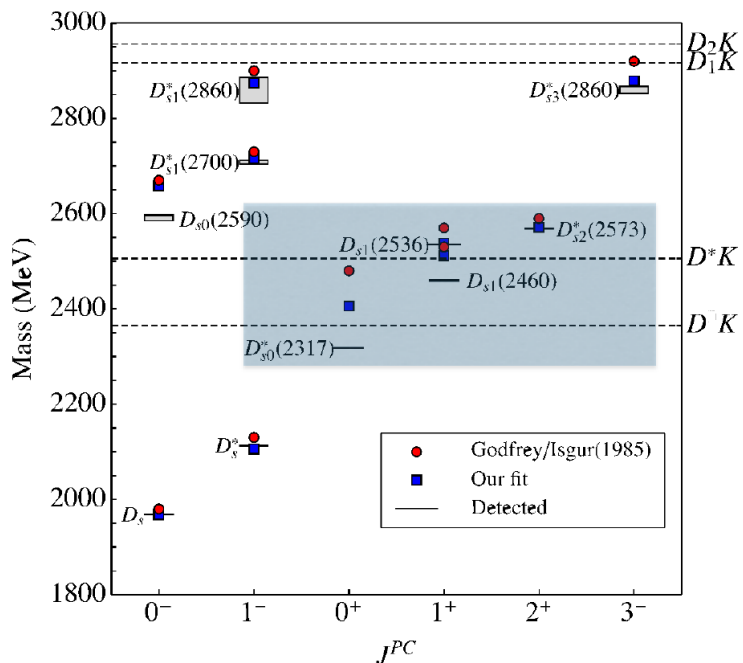
Z. Yang, G.-J. Wang, J.-j. Wu, S.-l. Zhu, M. Oka [Phys.Rev.Lett.128\(2022\),112001](#)



$D_{s0}(2317)$, $D_{s1}(2460)$, $D_{s1}(2536)$, $D_{s2}(2573)$

Z. Yang, G.-J. Wang, J.-j. Wu, S.-I. Zhu, M. Oka [Phys.Rev.Lett.128\(2022\),112001](#)

1. Fix the bare mass and wave function from GI model;



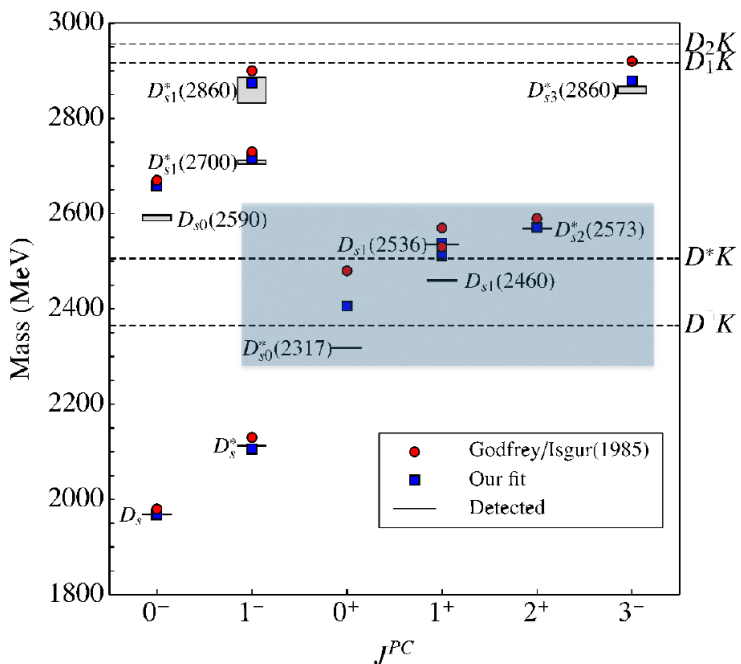
	$\bar{c}s$ cores	channel		
	$B(^{2S+1}L_J\rangle)$	$B(\text{mass})$	α	L
$D_{s0}^*(2317)$	$ ^3P_0\rangle$	2405.9	DK	S
$D_{s1}^*(2460)$	$0.68 ^1P_1\rangle - 0.74 ^3P_1\rangle$ $= -0.99\phi_s + 0.13\phi_d$	2511.5	D^*K	S, D
$D_{s1}^*(2536)$	$-0.74 ^1P_1\rangle - 0.68 ^3P_1\rangle$ $= -0.13\phi_s - 0.99\phi_d$	2537.8	D^*K	S, D
$D_{s2}^*(2573)$	$ ^3P_2\rangle$	2571.2	DK, D^*K	D



$D_{s0}(2317)$, $D_{s1}(2460)$, $D_{s1}(2536)$, $D_{s2}(2573)$

Z. Yang, G.-J. Wang, J.-j. Wu, S.-I. Zhu, M. Oka [Phys.Rev.Lett.128\(2022\),112001](#)

1. Fix the bare mass and wave function from GI model;
2. The interaction of bare-channel and channel-channel;



3P_0 model
at quark level

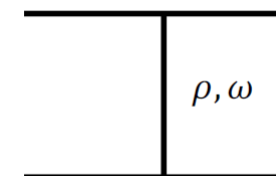
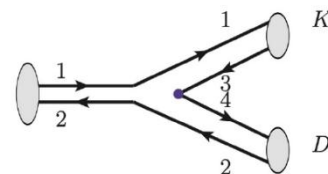


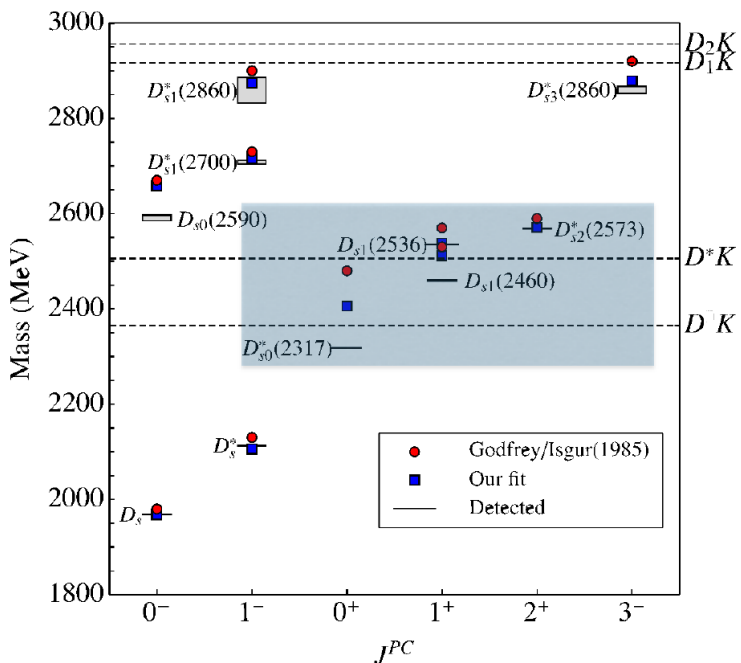
Figure 2: The diagram contribute to the process $D_s^*(2317) \rightarrow DK$.

	$\bar{c}s$ cores	$B(\text{mass})$	channel	
	$B(^{2S+1}L_J\rangle)$		α	L
$D_{s0}^*(2317)$	$ ^3P_0\rangle$	2405.9	DK	S
$D_{s1}^*(2460)$	$0.68 ^1P_1\rangle - 0.74 ^3P_1\rangle$ $= -0.99\phi_s + 0.13\phi_d$	2511.5	D^*K	S, D
$D_{s1}^*(2536)$	$-0.74 ^1P_1\rangle - 0.68 ^3P_1\rangle$ $= -0.13\phi_s - 0.99\phi_d$	2537.8	D^*K	S, D
$D_{s2}^*(2573)$	$ ^3P_2\rangle$	2571.2	DK, D^*K	D



$D_{s0}(2317)$, $D_{s1}(2460)$, $D_{s1}(2536)$, $D_{s2}(2573)$

Z. Yang, G.-J. Wang, J.-j. Wu, S.-I. Zhu, M. Oka *Phys.Rev.Lett.*128(2022),112001



	$\bar{c}s$ cores		channel	
	$B(^{2S+1}L_J\rangle)$	$B(\text{mass})$	α	L
$D_{s0}^*(2317)$	$ ^3P_0\rangle$	2405.9	DK	S
$D_{s1}^*(2460)$	$0.68 ^1P_1\rangle - 0.74 ^3P_1\rangle$ $= -0.99\phi_s + 0.13\phi_d$	2511.5	D^*K	S, D
$D_{s1}^*(2536)$	$-0.74 ^1P_1\rangle - 0.68 ^3P_1\rangle$ $= -0.13\phi_s - 0.99\phi_d$	2537.8	D^*K	S, D
$D_{s2}^*(2573)$	$ ^3P_2\rangle$	2571.2	DK, D^*K	D

1. Fix the bare mass and wave function from GI model;
2. The interaction of bare-channel and channel-channel;

3P_0 model
at quark level

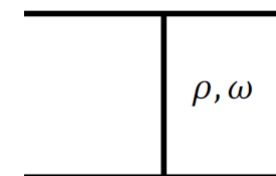
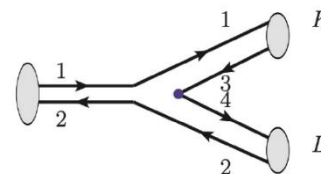
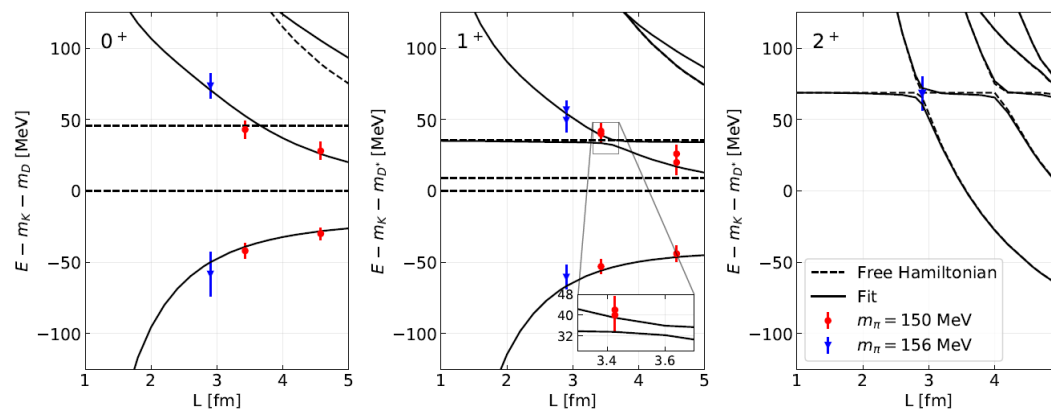


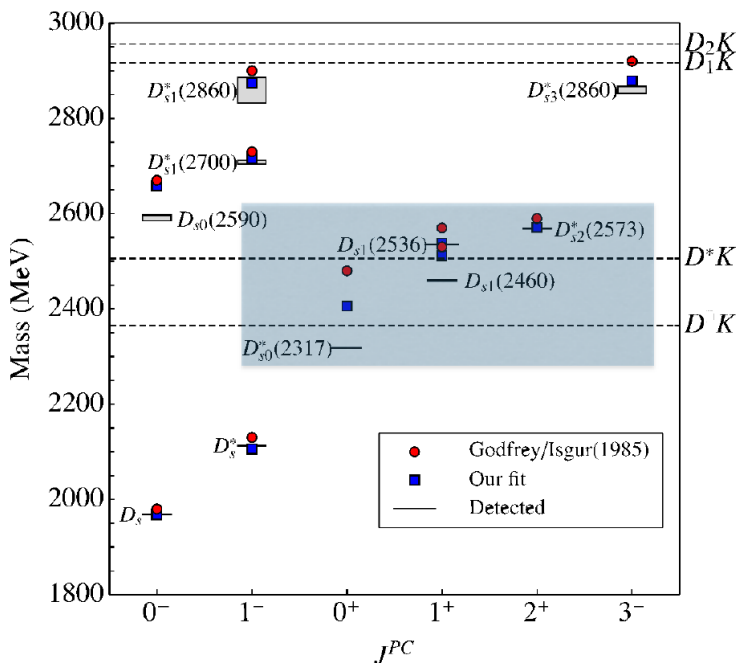
Figure 2: The diagram contribute to the process $D_s^*(2317) \rightarrow DK$.

3. Fit Lattice data;



$D_{s0}(2317)$, $D_{s1}(2460)$, $D_{s1}(2536)$, $D_{s2}(2573)$

Z. Yang, G.-J. Wang, J.-j. Wu, S.-I. Zhu, M. Oka *Phys.Rev.Lett.*128(2022),112001



	$\bar{c}s$ cores		channel	
	$B(^{2S+1}L_J\rangle)$	$B(\text{mass})$	α	L
$D_{s0}^*(2317)$	$ ^3P_0\rangle$	2405.9	DK	S
$D_{s1}^*(2460)$	$0.68 ^1P_1\rangle - 0.74 ^3P_1\rangle$ $= -0.99\phi_s + 0.13\phi_d$	2511.5	D^*K	S, D
$D_{s1}^*(2536)$	$-0.74 ^1P_1\rangle - 0.68 ^3P_1\rangle$ $= -0.13\phi_s - 0.99\phi_d$	2537.8	D^*K	S, D
$D_{s2}^*(2573)$	$ ^3P_2\rangle$	2571.2	DK, D^*K	D

1. Fix the bare mass and wave function from GI model;
2. The interaction of bare-channel and channel-channel;

3P_0 model
at quark level

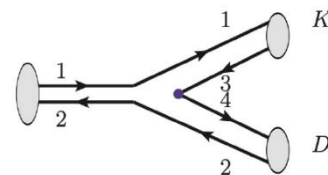
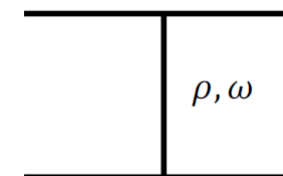
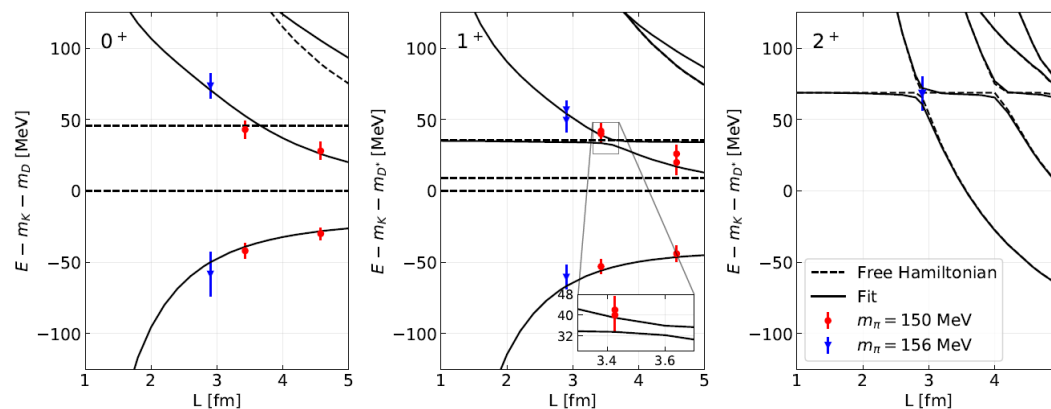


Figure 2: The diagram contribute to the process $D_s^*(2317) \rightarrow DK$.



	$P(c\bar{s})$
$D_{s0}^*(2317)$	$\approx 32.0\%$
$D_{s1}^*(2460)$	$\approx 52.4\%$
$D_{s1}^*(2536)$	$\approx 98.2\%$
$D_{s2}^*(2573)$	$\approx 95.9\%$

3. Fit Lattice data;



Conclusion:

$D_{s0}^*(2317)$ -DK S-wave
 $D_{s1}^*(2460)$ - D^*K

Mass moving vs GI Model

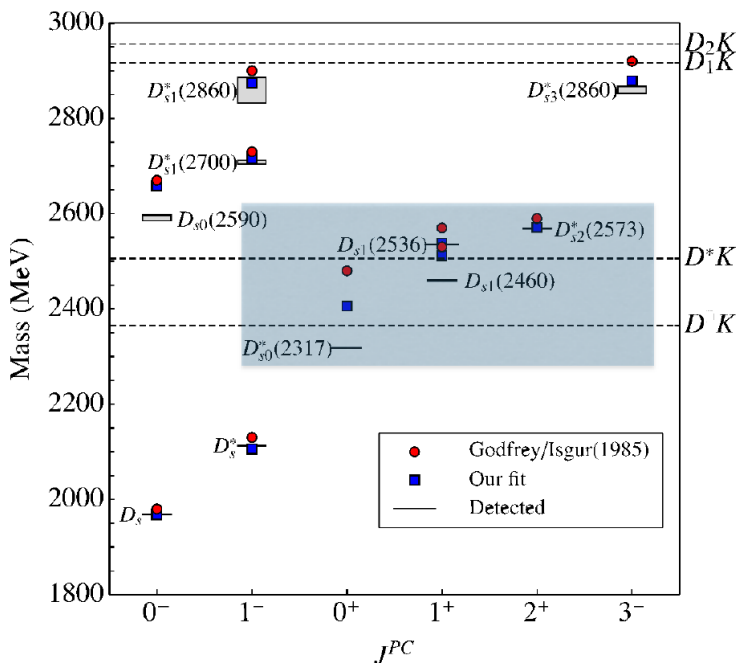
$D_{s1}^*(2536)$ - D^*K D-wave
 $D_{s2}^*(2573)$ - $D^{(*)}K$

Mass stable vs GI model

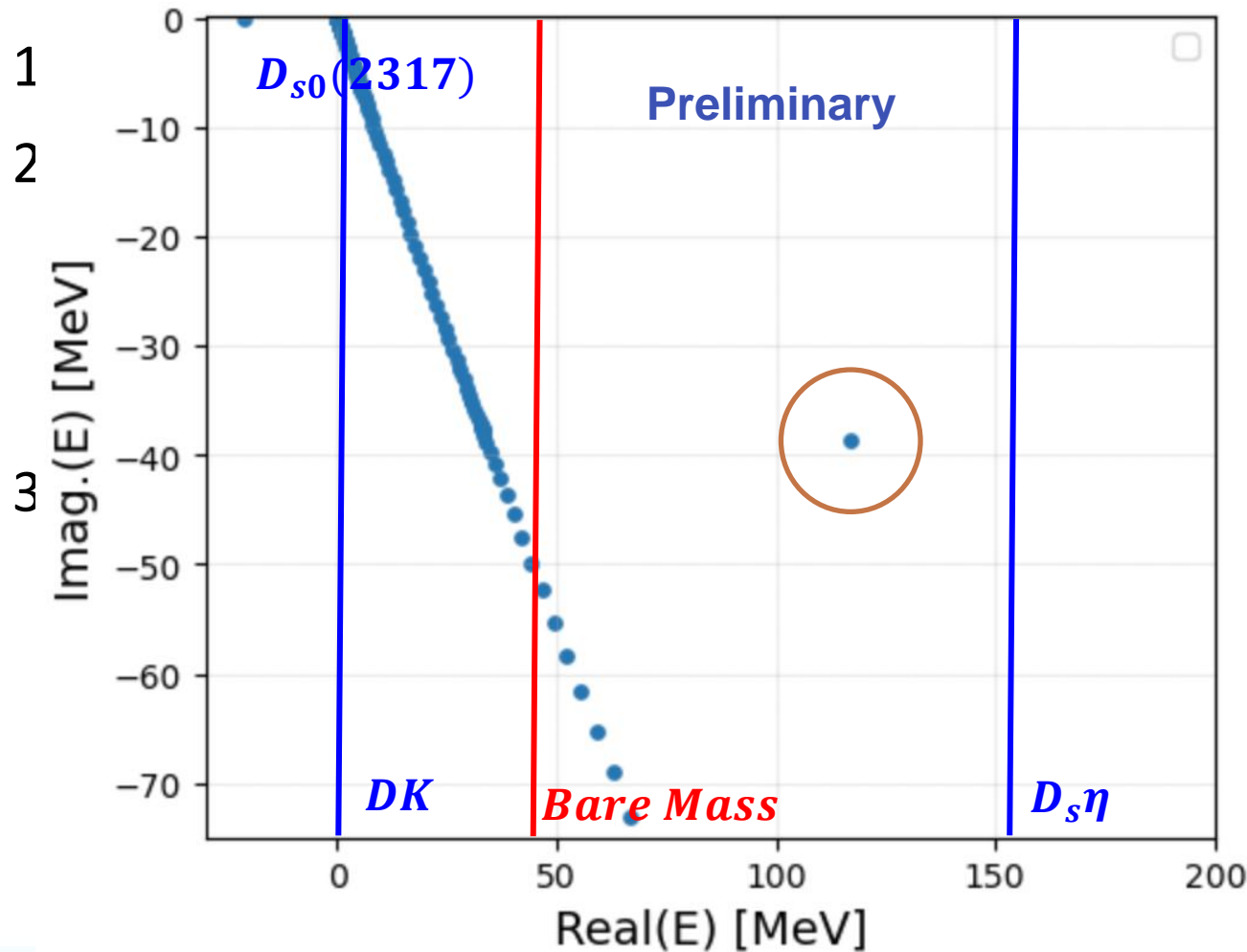


$D_{s0}(2317)$, $D_{s1}(2460)$, $D_{s1}(2536)$, $D_{s2}(2573)$

128(2022),112001



	$\bar{c}s$ cores		channel	
	$B(^{2S+1}L_J\rangle)$	$B(\text{mass})$	α	L
$D_{s0}^*(2317)$	$ ^3P_0\rangle$	2405.9	DK	S
$D_{s1}^*(2460)$	$0.68 ^1P_1\rangle - 0.74 ^3P_1\rangle$ $= -0.99\phi_s + 0.13\phi_d$	2511.5	D^*K	S, D
$D_{s1}^*(2536)$	$-0.74 ^1P_1\rangle - 0.68 ^3P_1\rangle$ $= -0.13\phi_s - 0.99\phi_d$	2537.8	D^*K	S, D
$D_{s2}^*(2573)$	$ ^3P_2\rangle$	2571.2	DK, D^*K	D



i

$-$

$-$

n :

1P_1 -DK

1D_2 - D^*K

fitting vs GI Model

1D_2 - D^*K

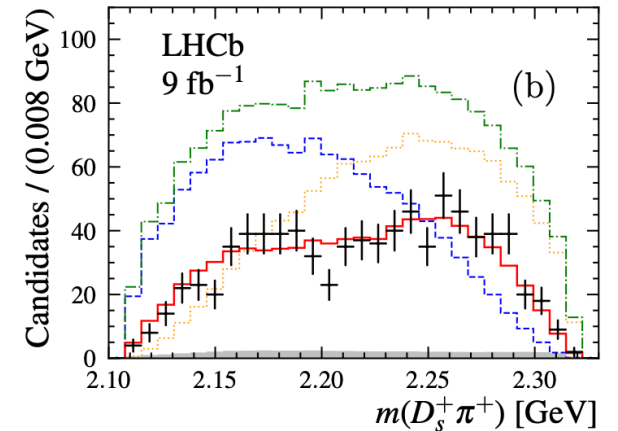
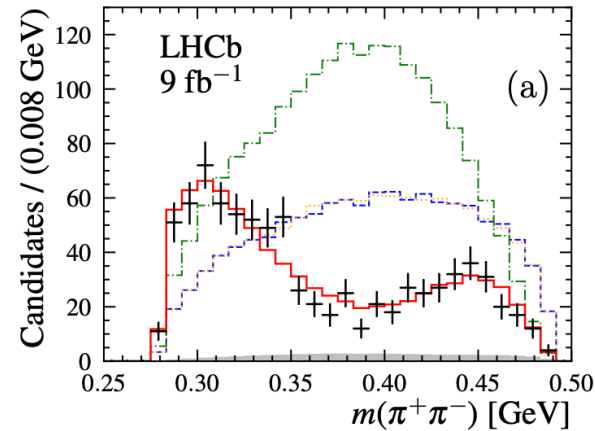
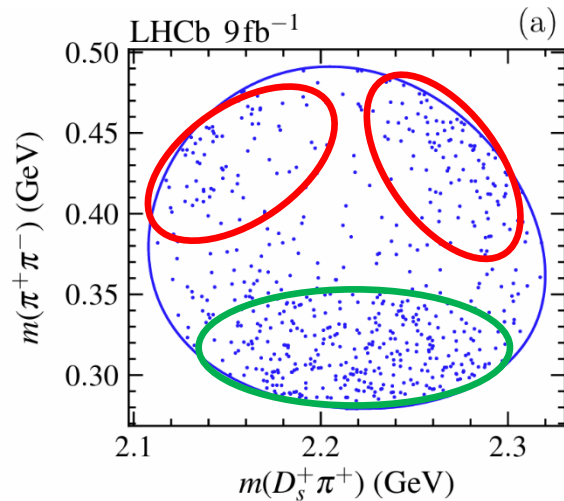
1D_2 - $D^{(*)}K$ D-wave

fitting vs GI model

15



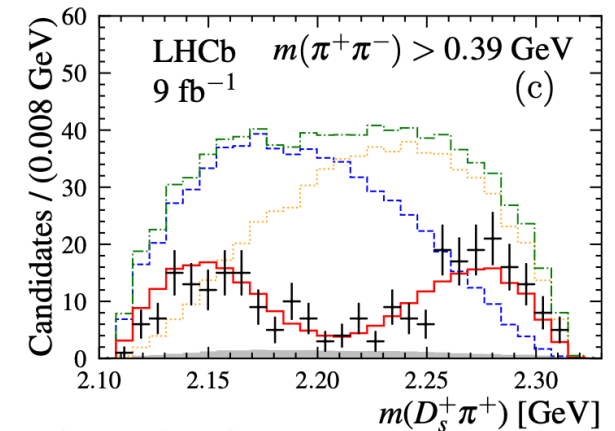
$B \rightarrow D^{(*)} D_{s1}(2460) \rightarrow D^{(*)} D_S^+ \pi^+ \pi^-$ decays



$D_S \rightarrow D_S \pi$ Isospin breaking
 $D_S^+ \pi^+, D_S^+ \pi^0, D_S^+ \pi^-$ are isospin triplet
 – Four quark state

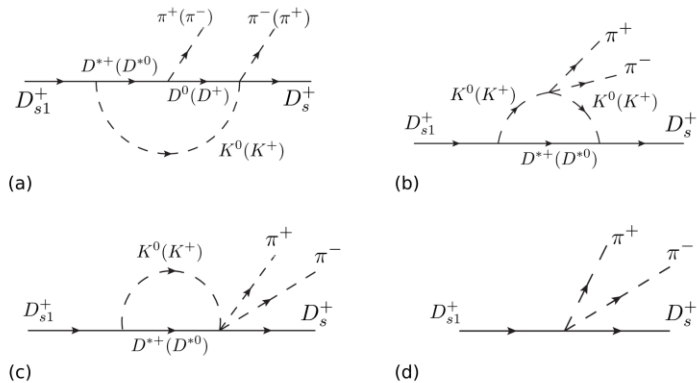
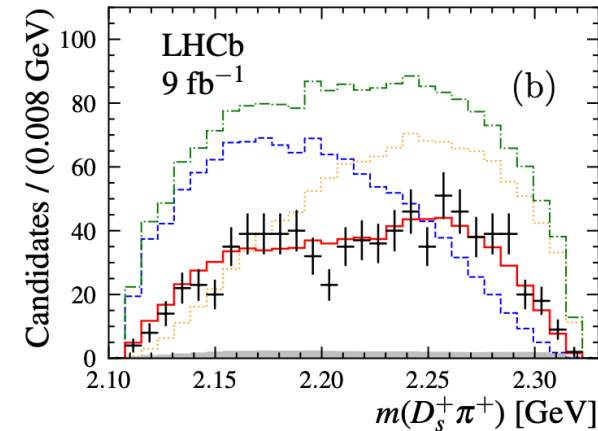
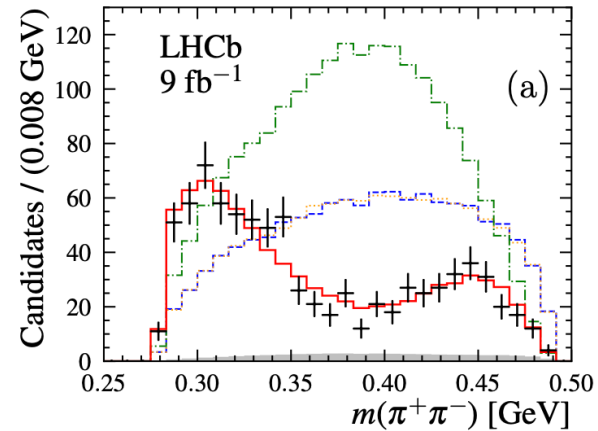
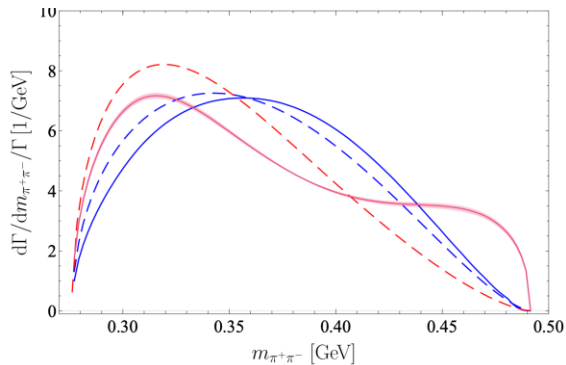
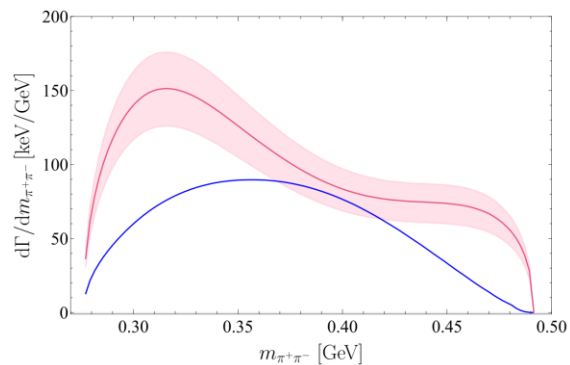
Model	Resonance	Mass (MeV)	Width (MeV)
$f_0(500) + \text{RBW } T_{c\bar{s}}(0^+)$	$f_0(500)$	$464 \pm 23 \pm 14$	$214 \pm 28 \pm 8$
	$T_{c\bar{s}}^{++}/T_{c\bar{s}}^0$	$2312 \pm 27 \pm 11$	$264 \pm 46 \pm 21$
$f_0(500) + \text{K-matrix } T_{c\bar{s}}(0^+)$	$f_0(500)$	$472 \pm 32 \pm 19$	$226 \pm 24 \pm 18$
	$T_{c\bar{s}}^{++}/T_{c\bar{s}}^0$	$2328 \pm 12 \pm 12$	$96 \pm 16 \pm 23$

- $T_{c\bar{s}}^{++}$
- $T_{c\bar{s}}^0$
- $f_0(500)$
- Background
- Total fit
- + Data



LHCb Sci.Bull. 70 (2025) 1432

$B \rightarrow D^{(*)} D_{s1}(2460) \rightarrow D^{(*)} D_s^+ \pi^+ \pi^-$ decays



**Tang, Lin, Guo,
Hanhart and Meissner,
Commun. Theor. Phys.
75 (2023)5 055203**

- $T_{c\bar{s}}^{++}$
- $T_{c\bar{s}}^0$
- $f_0(500)$
- Background
- Total fit
- + Data

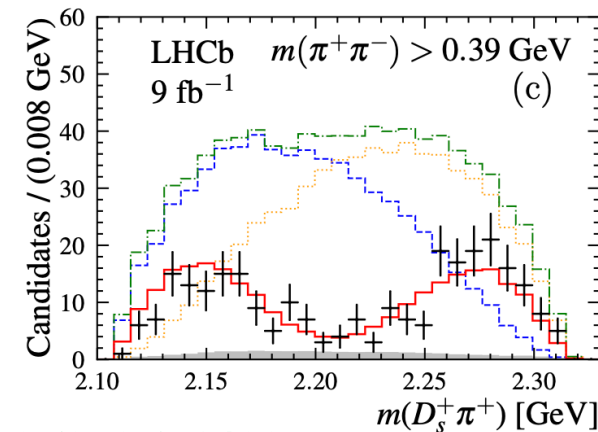
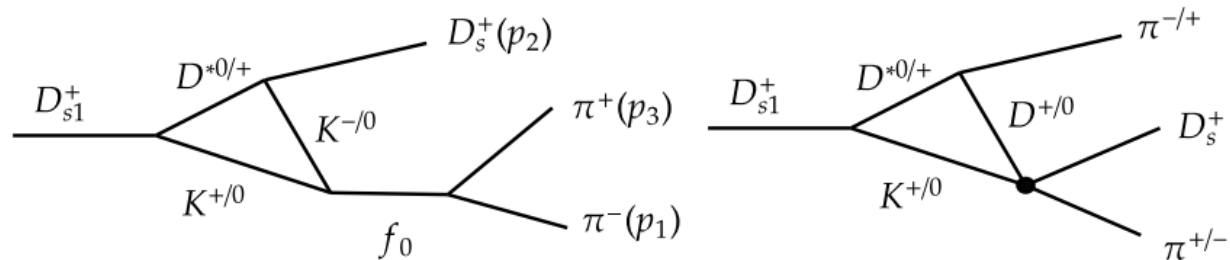


Figure 1. Diagrams for the decay $D_{s1}(2460)^+ \rightarrow D_s^+ \pi^+ \pi^-$ with (a+b+c) and without (d) the D^*K contribution.

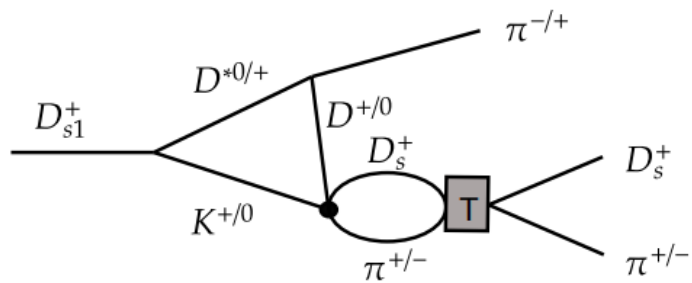
LHCb Sci.Bull. 70 (2025) 1432

$$D_{s1}(2460) \rightarrow D_s^+ \pi^+ \pi^-$$



(a)

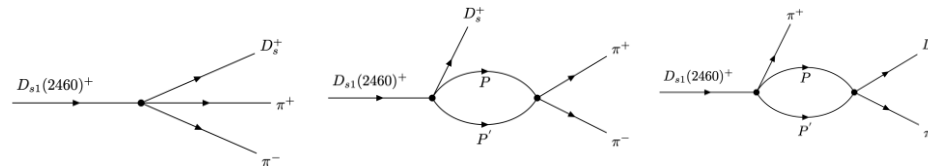
(b)



(c)

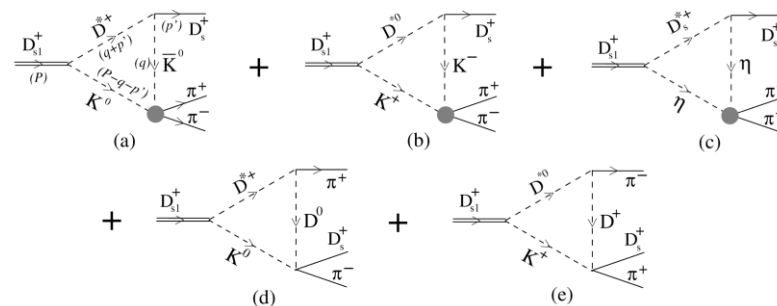
Z. Yang, G.-J. Wang, J.-J. Wu, M. Oka, 2510.01564

ZY Wang, YS Li and SQ Luo, PRD 111 (2025) 7, 076009



Missing the triangle loop, losing the nature of $D_{s1}(2460)$

Roca, Dias and Oset, Eur.Phys.J.C 85 (2025) 7, 808



Missing the coupled channel effect of $D_s \pi - DK$

$$D_{s1} \rightarrow D_S^+ \pi^+ \pi^-$$

$$L_\mu = P_{\mu\nu}(p_2 + q, m_{D^*})(q - p_2)^\nu,$$

$$N_\mu = P_{\mu\nu}(p_1 + q, m_{D^*})(p_1 - q)^\nu (p_2 - q + 2p_3)^\alpha$$

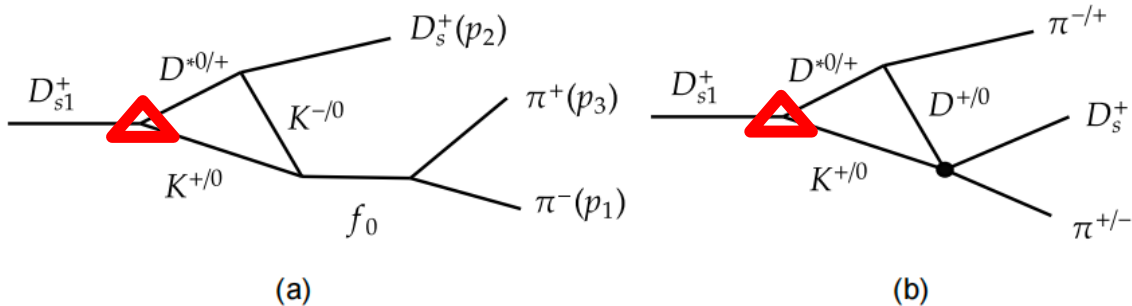
$$\times P_{\alpha\beta}(p_2 - q, m_{K^*})(p_2 + q)^\beta,$$

$$\mathcal{M} = \mathcal{M}_a + e^{i\phi}(\mathcal{M}_b + \mathcal{M}_c)$$

$$i\mathcal{M}_a = \frac{r_1}{m_{13}^2 - m_{f_0}^2 + im_{f_0}\Gamma_{f_0}} \int \frac{d^4q}{(2\pi)^4} \frac{\epsilon^\mu L_\mu}{[q^2 - m_K^2][(q + p_2)^2 - m_{D^*}^2][(p_0 - p_2 - q)^2 - m_K^2]},$$

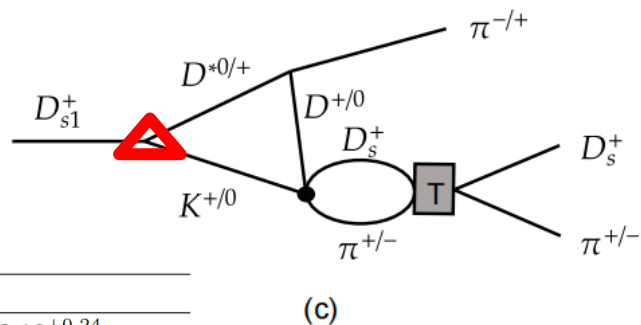
$$i\mathcal{M}_b = r_2 \int \sqrt{\pi} \sin\theta d\theta \int \frac{d^4q}{(2\pi)^4} \frac{\epsilon^\mu N_\mu}{[q^2 - m_D^2][(q + p_1)^2 - m_{D^*}^2][(p_0 - p_1 - q)^2 - m_K^2]} + (p_1 \leftrightarrow p_3),$$

$$i\mathcal{M}_c = r_2 \int \frac{\sin\theta d\theta k^2 dk}{2\pi^{3/2}} \int \frac{d^4q}{(2\pi)^4} \frac{\epsilon^\mu N_\mu G_{D_s\pi}(k, m_{23}) T_{D_s\pi \rightarrow D_s\pi}(k, p_{0n}, m_{23})}{[q^2 - m_D^2][(q + p_1)^2 - m_{D^*}^2][(p_0 - p_1 - q)^2 - m_K^2]} + (p_1 \leftrightarrow p_3),$$



(a)

(b)



(c)

Parameter	
Λ_1 [GeV]	$2.18_{-0.04}^{+0.24}$
Λ_2 [GeV]	0.5 (fixed)
g_{K^*}	$55.3_{-2.5}^{+0.8}$
ϕ [Rad]	$3.78_{-0.26}^{+0.38}$
r_1	215_{-86}^{+51}
r_2	$-9.0_{-0.8}^{+4.3}$
m_{f_0} [MeV]	519_{-89}^{+31}
Γ_{f_0} [MeV]	242_{-88}^{+90}
$\chi^2/\text{d.o.f.}$	1.43
E_p [MeV]	$2288.4_{-13.4}^{+11.7} - 89.6_{-6.4}^{+6.5}i$

Conclusion:

$D_{s0}^*(2317)$ -DK

$D_{s1}(2460)$ - D^*K

S-wave

Mass moving vs GI Model

$D_{s1}(2536)$ - D^*K

$D_{s2}(2573)$ - $D^{(*)}K$

D-wave

Mass stable vs GI model

$$\mathcal{M}_S = g_S \epsilon_i^\mu \epsilon_{j,\mu}^\dagger$$

$$\mathcal{M}_D = \frac{g_D}{M^2} \epsilon_i^\mu \epsilon_j^{\dagger\nu} \left(q_\mu q_\nu - \frac{g_{\mu\nu} q^2}{4} \right)$$

$$D_{s1}(2460): g_S \gg g_D$$

$$D_{s1}(2536): \frac{g_S}{g_D} = 0.08 e^{2.67i}$$

LHCb, JHEP 10 (2023) 106

$$\frac{g_S}{g_D} = 0.1 e^{-0.7i}$$

Elegant model.

1. We successfully combine two D_{s1} states together.
2. Various free parameters are combined together.
3. We seriously consider the T matrix of $D_S\pi - DK$ scattering.



$$D_{s1} \rightarrow D_S^+ \pi^+ \pi^-$$

$$L_\mu = P_{\mu\nu}(p_2 + q, m_{D^*})(q - p_2)^\nu,$$

$$N_\mu = P_{\mu\nu}(p_1 + q, m_{D^*})(p_1 - q)^\nu (p_2 - q + 2p_3)^\alpha$$

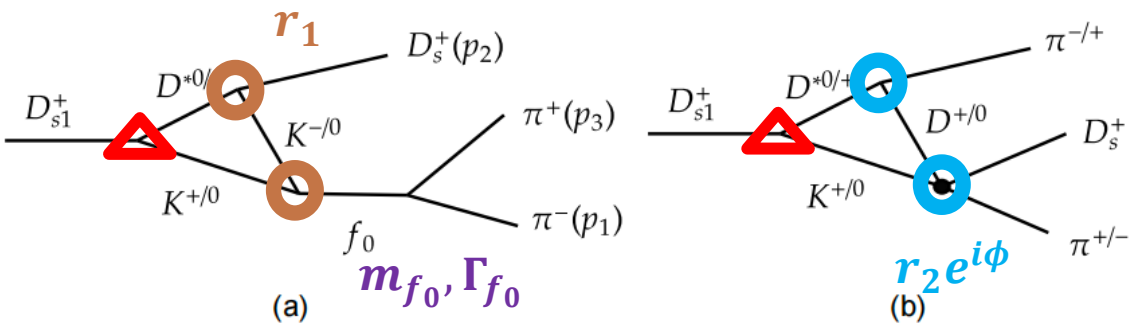
$$\times P_{\alpha\beta}(p_2 - q, m_{K^*})(p_2 + q)^\beta,$$

$$\mathcal{M} = \mathcal{M}_a + e^{i\phi}(\mathcal{M}_b + \mathcal{M}_c)$$

$$i\mathcal{M}_a = \frac{r_1}{m_{13}^2 - m_{f_0}^2 + im_{f_0}\Gamma_{f_0}} \int \frac{d^4q}{(2\pi)^4} \frac{\epsilon^\mu L_\mu}{[q^2 - m_K^2][(q + p_2)^2 - m_{D^*}^2][(p_0 - p_2 - q)^2 - m_K^2]},$$

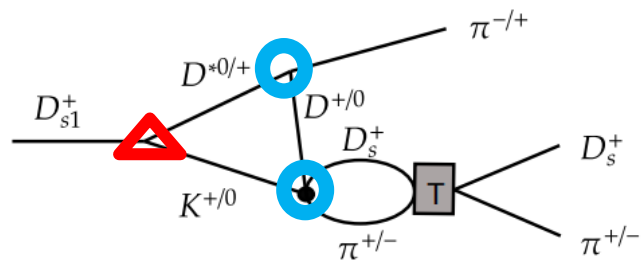
$$i\mathcal{M}_b = r_2 \int \sqrt{\pi} \sin\theta d\theta \int \frac{d^4q}{(2\pi)^4} \frac{\epsilon^\mu N_\mu}{[q^2 - m_D^2][(q + p_1)^2 - m_{D^*}^2][(p_0 - p_1 - q)^2 - m_K^2]} + (p_1 \leftrightarrow p_3),$$

$$i\mathcal{M}_c = r_2 \int \frac{\sin\theta d\theta k^2 dk}{2\pi^{3/2}} \int \frac{d^4q}{(2\pi)^4} \frac{\epsilon^\mu N_\mu G_{D_s\pi}(k, m_{23}) T_{D_s\pi \rightarrow D_s\pi}(k, p_{0n}, m_{23})}{[q^2 - m_D^2][(q + p_1)^2 - m_{D^*}^2][(p_0 - p_1 - q)^2 - m_K^2]} + (p_1 \leftrightarrow p_3),$$



(a) m_{f_0}, Γ_{f_0}

(b) $r_2 e^{i\phi}$



(c) $\Lambda_1, \Lambda_2, g_{K^*}$

Parameter	
Λ_1 [GeV]	$2.18^{+0.24}_{-0.04}$
Λ_2 [GeV]	0.5 (fixed)
g_{K^*}	$55.3^{+0.8}_{-2.5}$
ϕ [Rad]	$3.78^{+0.38}_{-0.26}$
r_1	215^{+51}_{-86}
r_2	$-9.0^{+4.3}_{-0.8}$
m_{f_0} [MeV]	519^{+31}_{-89}
Γ_{f_0} [MeV]	242^{+90}_{-88}
$\chi^2/\text{d.o.f.}$	1.43
E_p [MeV]	$2288.4^{+11.7}_{-13.4} - 89.6^{+6.5}_{-6.4}i$

Conclusion:

$D_{s0}^*(2317)$ -DK

$D_{s1}(2460)$ - D^*K

S-wave

Mass moving vs GI Model

$D_{s1}(2536)$ - D^*K

$D_{s2}(2573)$ - $D^{(*)}K$

D-wave

Mass stable vs GI model

$$\mathcal{M}_S = g_S \epsilon_i^\mu \epsilon_{j,\mu}^\dagger$$

$$\mathcal{M}_D = \frac{g_D}{M^2} \epsilon_i^\mu \epsilon_j^{\dagger\nu} \left(q_\mu q_\nu - \frac{g_{\mu\nu} q^2}{4} \right)$$

$$D_{s1}(2460): g_S \gg g_D$$

$$D_{s1}(2536): \frac{g_S}{g_D} = 0.08 e^{2.67i}$$

LHCb, JHEP 10 (2023) 106

$$\frac{g_S}{g_D} = 0.1 e^{-0.7i}$$

Elegant model.

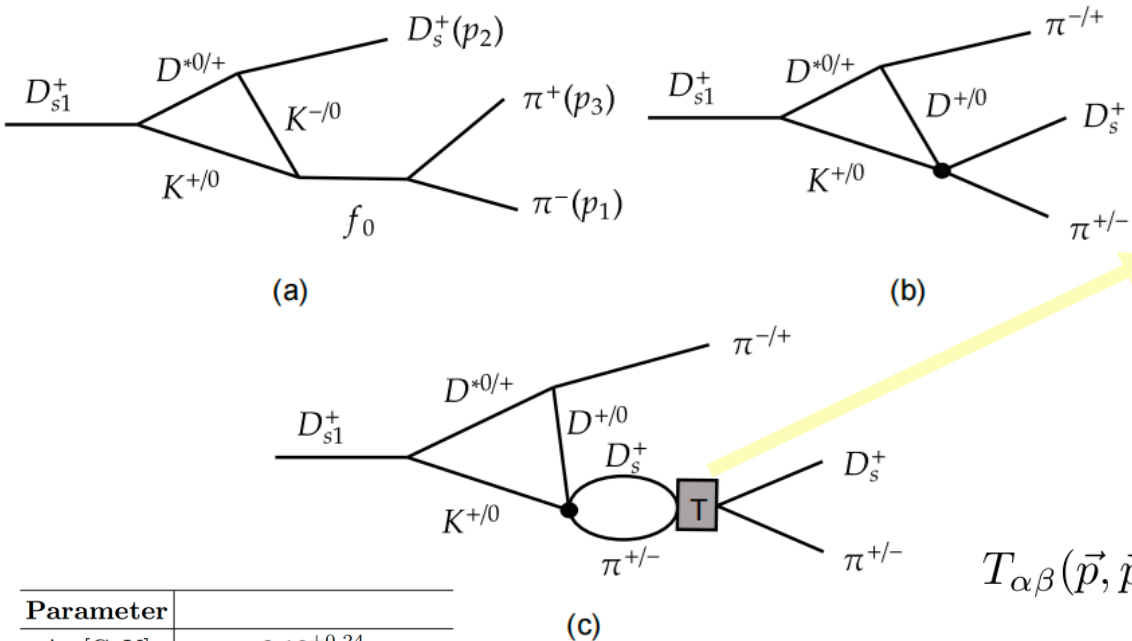
1. We successfully combine two D_{s1} states together.

2. **Various free parameters are combined together.**

3. We seriously consider the T matrix of $D_S\pi - DK$ scattering.



$D_{s1} \rightarrow D_s^+ \pi^+ \pi^-$



K^0	K^0	$I = 0, V_\rho + V_\omega < 0$	π^+	π^+	$V \sim 0$
D^+	D^+	$I = 1, V_\rho - V_\omega \sim 0$	D_s^+	D_s^+	
K^+	π^+	$V \neq 0$	π^+	π^+	$T = (1 - VG)^{-1}V$ $\rightarrow \det T^{-1} \propto (1 - V^2 G_{DK} G_{D_S\pi})$
D^+	D_s^+		K^{*0}	D_s^+	

For DK , effective potential is $V^2 G_{D_S\pi}$
 For $D_S\pi$, effective potential is $V^2 G_{DK}$
 Control the value of cut off will adjust the effective potential.

Parameter	
Λ_1 [GeV]	$2.18^{+0.24}_{-0.04}$
Λ_2 [GeV]	0.5 (fixed)
g_{K^*}	$55.3^{+0.8}_{-2.5}$
ϕ [Rad]	$3.78^{+0.38}_{-0.26}$
r_1	215^{+51}_{-86}
r_2	$-9.0^{+4.3}_{-0.8}$
m_{f_0} [MeV]	519^{+31}_{-89}
Γ_{f_0} [MeV]	242^{+90}_{-88}
$\chi^2/\text{d.o.f.}$	1.43
E_p [MeV]	$2288.4^{+11.7}_{-13.4} - 89.6^{+6.5}_{-6.4}i$

$$T_{\alpha\beta}(\vec{p}, \vec{p}'; E) = \mathcal{V}_{\alpha\beta}(\vec{p}, \vec{p}'; E) + \sum_{\gamma} \int d\vec{q} \frac{\mathcal{V}_{\alpha\gamma}(\vec{p}, \vec{q}; E) T_{\gamma\beta}(\vec{q}, \vec{p}'; E)}{E - \sqrt{m_{\gamma_1}^2 + q^2} - \sqrt{m_{\gamma_2}^2 + q^2} + i\epsilon}$$

$$\mathcal{V} = \frac{g_{K^*} (p_\pi + p_K) \cdot (p_{D_s} + p_D)}{(p_\pi - p_K)^2 - m_{K^*}^2} \left(\frac{\Lambda_1^2}{\Lambda_1^2 + p_1^2} \frac{\Lambda_2^2}{\Lambda_2^2 + p_2^2} \right)$$

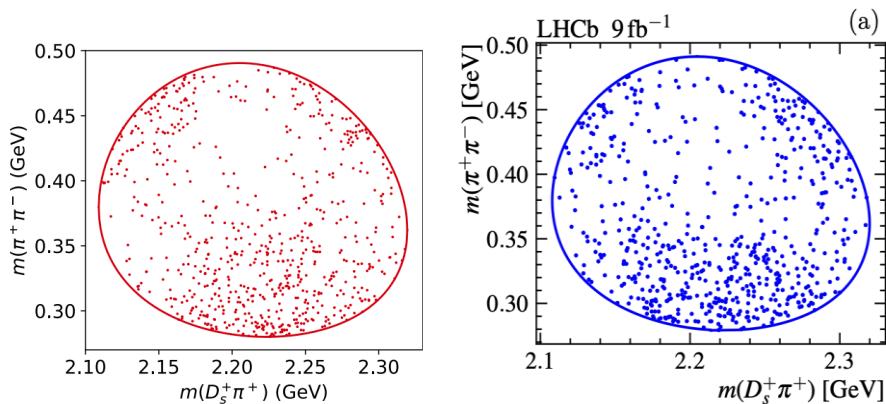
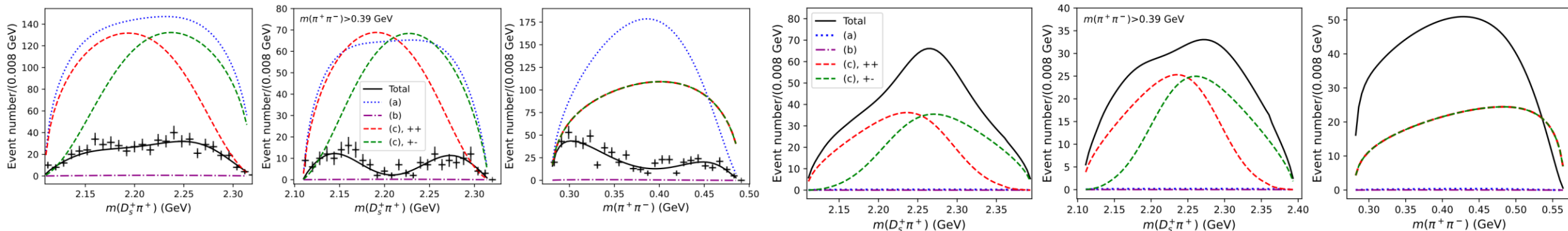
Elegant model.

1. We successfully combine two D_{s1} states together.
2. Various free parameters are combined together.
3. We seriously consider the T matrix of $D_S\pi - DK$ scattering.

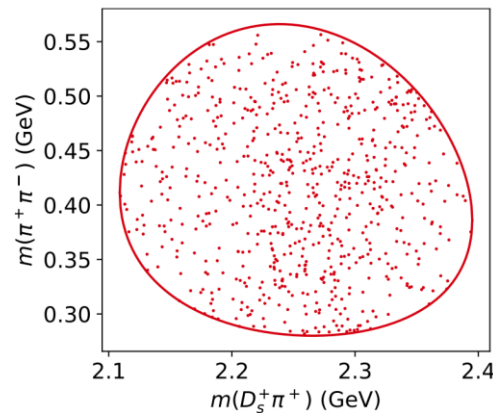
$$D_{s1} \rightarrow D_s^+ \pi^+ \pi^-$$

$D_{s1}(2460)$

$D_{s1}(2536)$



χ^2 / dof
= 1.43



If a stricter cut is applied, for instance, $m(\pi^+ \pi^-) > 0.45$ GeV, the two-peak structure will appear.

Z. Yang, G.-J. Wang, J.-J. Wu, M. Oka, 2510.01564

Summary

- The strong interaction involves physics at two distinct levels and is extremely complex.
- We introduce the **NonPerturbative Hamiltonian Framework** (NPHF) approach, which connects the quark-gluon level to the hadronic level via a bare state, establishing a coupled-channel model with varying numbers of hadrons to achieve a comprehensive understanding of hadron properties.
- Using lattice QCD data, we explain why the masses of D_{s0} (2317) and D_{s1} (2460) are lower than predictions from conventional quark models, while those of D_{s1} (2536) and D_{s2} (2573) agree well.
- It further elucidates the D_{s1} (2460) $\rightarrow D_s \pi \pi$, reveals the existence of the $T_{c\bar{s}}$ state, and predicts the D_{s1} (2536) $\rightarrow D_s \pi \pi$.

